Seventh International Conference on
Computational Fluid Dynamics (ICCFD7),
Big Island, Hawaii, July 9-13, 2012

ICCFD7-4401

Numerical Analysis of Stabilizing effect of Longitudinal Wall-Oscillation on Two Dimensional Channel Flow

T. Atobe
Corresponding author: atobe.takashi@jaxa.jp

Japan Aerospace Exploration Agency, JAPAN.

Abstract: The effect of longitudinal wall-oscillation for the stability of two dimensional channel flow is numerically investigated using the direct numerical simulation (DNS). In ordinary circumstances, the flow between two flat plates transits from laminar to turbulent state when the Reynolds number determined by typical quantities of the flow exceeds a critical value. With longitudinal wall-oscillation, however, it is found that the transition is accelerated or decelerated depending on the parameters of the wall-oscillation even if the Reynolds number is fixed to supercritical condition. From the flow visualization, it is clearly shown that the development of the streaks near the walls are suppressed by the wall-oscillation for the accelerated case. Also, the results obtained by the Floquet analysis support the features shown by the DNS.

Keywords: Channel flow, wall-oscillation, transition, stability, DNS, Floquet.

1   Introduction

Drag reduction is one of the most important issue on the public transport systems. For the aircraft, the account of skin friction in the total drag is relatively large. Intensity of the skin friction depends on condition of the boundary layer flow. In general, the skin friction is large when the boundary layer flow is turbulent. Thus, from the view point of the flow control, our interest is how to decrease the turbulent shear stress, or how to delay the laminar-turbulent transition.

In this context, investigation for the plane Poiseuille flow, so called the channel flow, is a realistic and useful example because it can be described as an exact solution of a linear equation derived from the Navier-Stokes equation, and some theoretical and numerical investigation have revealed its essential futures[1,2]. Thus there are various studies of the plane Poiseuille flow aiming at drag reduction. As for the passive control, wavy wall or roughness surface were investigated[3,4]. On the other hand, as active control, wavy walls, vibrating walls, or suction/blowing walls were examined[5-8].

As the study of the active control, Jung et al.[9] firstly pointed out about reduction of the wall shear stress for a turbulent channel flow due to spanwise wall-oscillation. Succeeded study by Quadrio and Ricco[10] numerically demonstrated the friction-drag reduction of 44.7%, which corresponds to the net energy saving of 7.3%. This modified flow not only has the advantage of the amount of the drag reduction, but also has an analogy with simple coupling of the channel flow with the Stokes layer. Thus, many efforts have been devoted to this problem[11,12].

Although this modified channel flow with spanwise wall-oscillation can be simplified based on the Stokes layer, its basic flow is fundamentally three dimensional flow. Thus, for the purpose of more simplification, modified channel flow with longitudinal wall-oscillation should be studied. From this view point, the authors focused on the stabilizing effect of the longitudinal wall-oscillation on the

plane Poiseuille flow. Since the Stokes layer is also an exact solution of the linear equation derived from the Navier-Stokes equation as same as the plane Poiseuille flow, this modified flow can be described a superposition of those two exact solutions. Therefore, the linear stability analysis based on the Floquet theory is applied together with the DNS. That is, the DNS can demonstrate detail character of the flow field and the Floquet analysis can show general feature of the system easily.

In Section 2, the results of the DNS study are presented. In Section 3, the study using the linear stability analysis based on the Floquet theory is described. Finally conclusions are given in Section 4.

2 Numerical Analysis
2.1 Two-Dimensional Channel Flow

Figure 1 shows a model flow considered. Here, Ω and U_w are frequency and amplitude of the longitudinal wall-oscillation. Thus, parameters describing this system are Ω, U_w, and the Reynolds number defined as $Re \equiv h\, U_{max}/\nu$, where U_{max} is the maximum value of the mean flow, ν the kinematic viscosity and h a half distance between two walls. In the present study, Re is fixed as 10000, which is a supercritical one, for convenience.
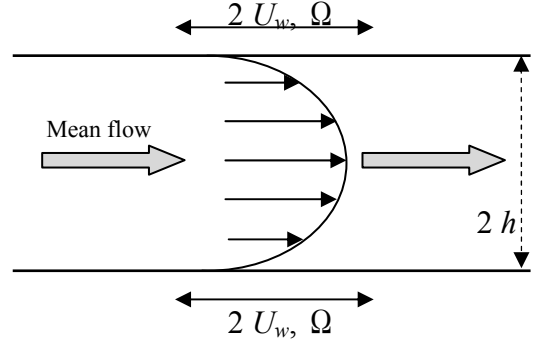
Fig.1 Schematic view of the modified channel flow.

The coordinate system of (x,y,z) corresponding to the physical space is taken for x in the streamwise direction, y in the direction normal to the wall, z in the spanwise direction. As mentioned before, the modified flow dealt here can be thought as a superposition of the exact solutions of a linear government equation as the follows,

$$\frac{\partial U}{\partial t} - \nu(\frac{\partial^2 U}{\partial y^2} + \frac{\partial^2 U}{\partial z^2}) = -\frac{1}{\rho}\frac{\partial p}{\partial x}, \qquad (1)$$

here ρ is the dencity. This equation is derived from the incompressible Navier-Stokes equation under the parallel flow assumption. In this context, the flow can be represented as $U=U(U(y,t),0,0)$, and $U(y,t)$ is,

$$U(y,t) = 1 - y^2 + U_w \operatorname{Re}[\frac{\cosh(ky)}{\cosh(k)}]\exp(i\Omega t), \quad (2)$$

here, $k \equiv \sqrt{\Omega/2\nu}$, and i denotes the imaginary unit. The former part of Eq.(2) is contribution of the plane Poiseuille flow, and the latter is the Stokes layer. In the Floquet analysis, Eq.(2) is used as the basic flow.

2.2 Direct Numerical Simulation

The numerical space is set as $x \in [0, 4\pi]$, $y \in [-1,1]$, $z \in [0, 2\pi]$. The flow filed is described as a superimposition of the disturbance $u=u(u,v,w)$ on the basic flow $U(y,t)$. If the pressure can be written as $-2x/Re + p$, the dimensionless equation for u is obtained from the Navier-Stokes equation,

$$\frac{\partial u}{\partial t} + U\frac{\partial u}{\partial x} + v\frac{\partial U}{\partial y}e_x = -\nabla \times u \times u - \nabla p + \frac{1}{Re}\nabla^2 u, \quad (3)$$

here, e_x denotes an unit vector in x the direction. The incompressible condition is,

$$\nabla \cdot u = 0. \qquad (4)$$

The velocity u is expanded by the Fourier series for x, z directions on the Chebyshev collocation points y_j.

$$u(x, y_j, z, t) = \sum_{k_x, k_z} u(k_x, y_j, k_z, t)\exp[i(k_x x + k_z z)]. \quad (5)$$

Then, Eq.(3) is calculated by the Fourier-Chebyshev spectral method[13] for $u(k_x, y_j, k_z, t)$ with the initial disturbances given as,

$$u(k_x, y_j, k_z, 0) = \varepsilon q(k_x, y_j, k_z), \qquad (6)$$

where ε is a small parameter and q is a random function which satisfied the solenoidal condition. Energy norm for the Fourier modes (k_x, k_z) per unit mass is defined as the follow.

$$E(k_x, k_z) \equiv \frac{1}{4} \int_{-1}^{1} |u(k_x, y, k_z)|^2 \, dy. \qquad (7)$$

2.3 Results

A typical results is shown in Fig.2 for the case of $(\Omega, U_w) = (0.0, 0.0)$ which corresponds to the genuine plane Poiseuille flow. The curves in this figure represent the time variation of energy for each Fourier mode $E(k_x, k_z)$. The solid lines correspond to two-dimensional disturbance, namely $E(k_x, 0)$, and the dotted lines correspond to three-dimensional ones. In this calculation, the simulation has been started with the initial disturbances of order 10^9, but a specific disturbance with relatively large amplitude of order 10^5. This large disturbance is a Fourier mode of $E(1,0)$, which is called the Tollmien-Schlichting (TS) wave. Because it is well known that the TS mode is dominant and leads to the laminar-turbulent transition under the flow condition considered here, the large TS mode is initially added to the initial disturbance in order to save the computing time-cost. In the present study, all of the simulation examined are including this TS mode.
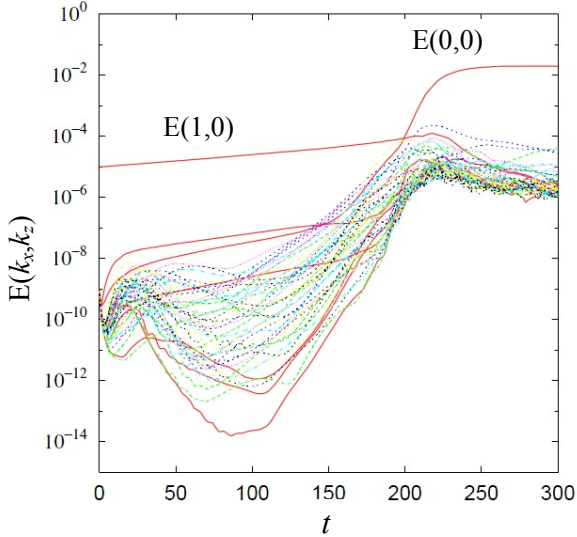

Fig. 2 Variation of energy for each Fourier mode for the case of $(\Omega, U_w) = (0,0)$
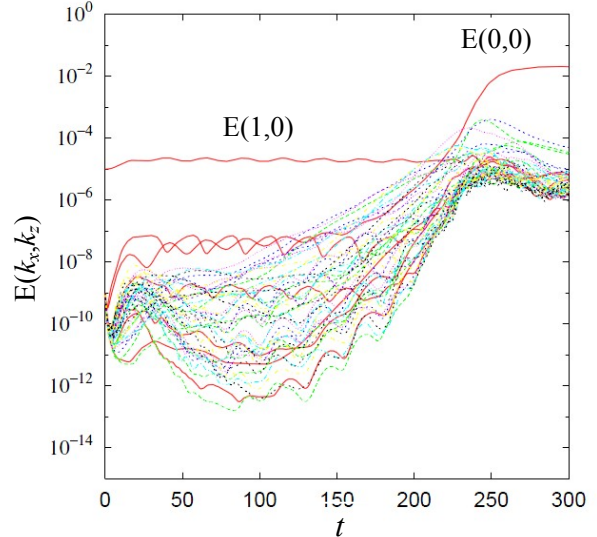
Fig. 3 Variation of energy for each Fourier mode for the case of $(\Omega, U_w) = (0.25, 0.3)$

From this figure, it can be seen that after the transient phase the energy of the each mode develop with time and the laminar-turbulent transition occurs at about t=230 in this case.

Some results with wall-oscillation are shown Fig.3-5 for the case of $(\Omega, U_w) = (0.25, 0.3)$, (0.05, 0.2), and (0.15, 0.2). The result of Fig.3 seems to almost same as non-oscillating case of Fig.2 except for oscillation in the time variation of the energy for each Fourier mode. It can be easily supposed that this oscillation is caused by the oscillation of the walls. Actually, it was confirmed that the period of the oscillation appearing on the time variation of the energy coincides with that of the wall-oscillation. In Fig.4, the laminar-turbulent transition is accelerated by the wall-oscillation. In this case, it takes only about 80 non-dimensional time for the transition. On the other hand, the result of the Fig.5, the transition to turbulent is slightly delayed by the wall oscillation.
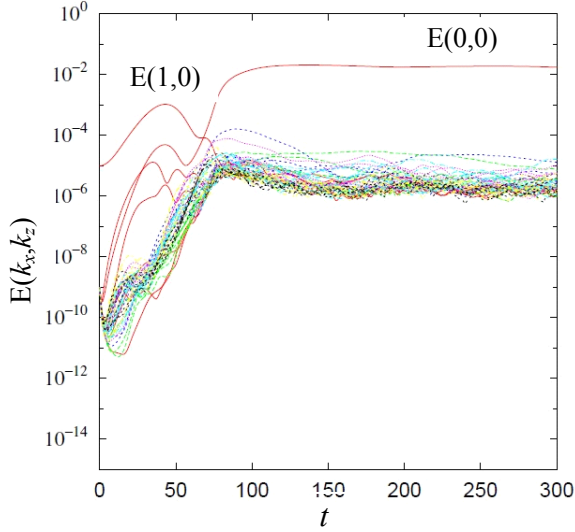
Fig. 4 Variation of energy for each Fourier mode for the case of (Ω, U_w)=(0.05,0.2)
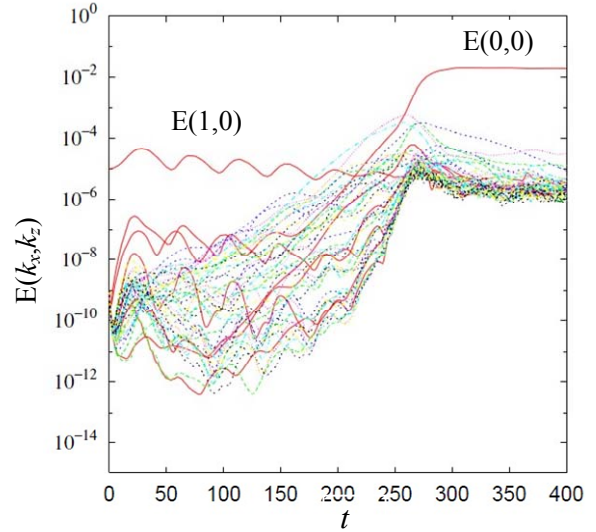

Fig. 5 Variation of energy for each Fourier mode for the case of (Ω, U_w)=(0.15,0.2)

It is found from such parametric study that the laminar-turbulent transition of the flow can roughly be grouped in three patterns depending on the wall-oscillation. Result of this parametric study is shown in Fig.6. The circles correspond to the accelerated cases, the diamonds to the decelerated, and square to the less affected cases. It seems that the accelerated cases exist in small Ω region.

Figure 7 shows a contour of instantaneous vorticity for (a) at t=150 of Fig.3, and (b) at t=50 of Fig.4. The white color corresponds to the streamwise components, and the dark color corresponds to spanwise components. In the case without wall-oscillation, relatively large scale coherent structures so called "streak" or "lambda shaped vortex" exists near the walls. However, at least at this instant, the small scale spanwise vortices exist instead of the streak. It might be conjectured that the absence of the streamwise coherent structure leads to the results of the acceleration of the transition.
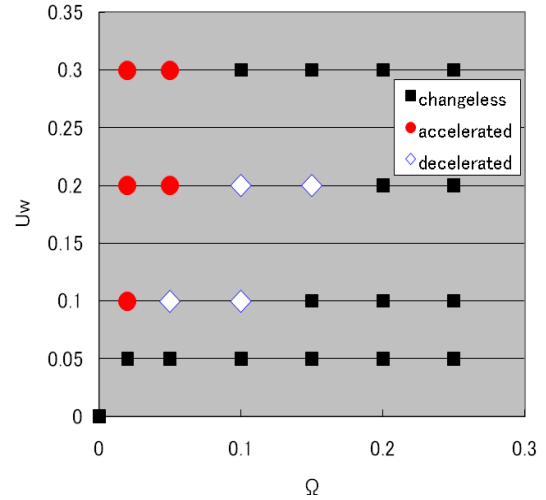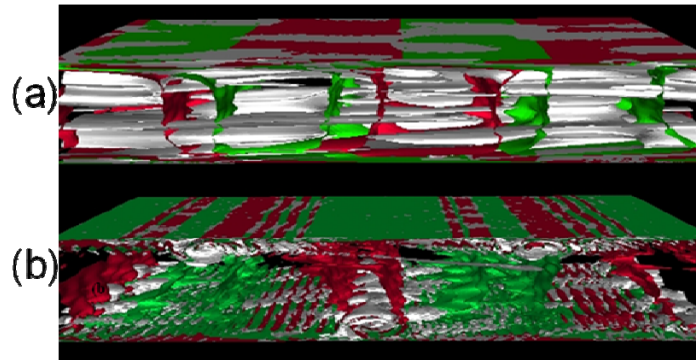

Fig. 6 Results of the parametric study.

Fig. 7 Flow visualization by the streamwise vorticity (represented by white contour).
(a) at t=150 of Fig.3. (b) at t=50 of Fig.4.

3 Floquet Analysis

3.1 Time-Dependent Ordinary Equation

When the flow field is described by the basic flow U and the small disturbance u' and p', the linearized disturbance equation for u' can be derived from the Navier-Stokes equation as the follows.

$$\frac{\partial u'}{\partial t} + (U \cdot \text{grad})u' + (u' \cdot \text{grad})U = -\frac{1}{\rho}\text{grad}\, p' + \nu\nabla^2 u'. \quad (8)$$

Now, we assume that the small disturbance can be described as a modal plane wave,

$$u'(x, y, z, t) = \hat{u}(y, t)\exp[i(\alpha x + \gamma z)], \quad (9)$$

here α, γ are real wave number in x, z direction, respectively. Substituting Eq.(9) into Eq.(8) with the equation of continuity, we obtain time-dependent Orr-sommerfeld equation, which takes the form of

$$[(\frac{\partial}{\partial t} + i\alpha U(y,t))(D^2 - \alpha^2 - \gamma^2) - i\alpha D^2 U(y,t)]\hat{v}(y,t)$$
$$= \frac{1}{R}(D^2 - \alpha^2 - \gamma^2)^2 \hat{v}(y,t) \quad , (10)$$

where D is the differential operator in y direction.

3.2 Floquet Exponet

If Eq.(10) can be rewritten as the form,

$$\frac{\partial}{\partial t}\hat{v}(y,t) = G(y,t)\hat{v}(y,t), \quad (11)$$

because of the periodicity of function G, we can expect from the Floquet theory that the solution of Eq.(11) can be described as the follows,

$$\hat{v}_i(y,t) = e^{\mu_i t}\phi_i(y,t), \quad (i=1,2,\cdots). \quad (12)$$

Here $\varphi_i(y,t)$ is a periodic function with the period T, and μ_i is a complex number called as Floquet exponents. If the real part of μ_i is positive, the system should be unstable.

Thus, in order to rewrite Eq.(10) as the form of Eq.(11), the Chebyshec spectral collocation method is employed. For this, Gauss-Lobatto scheme is adopted for the collocation points,

$$y_j = \cos\frac{\pi j}{N+1}, \quad (j=0,1,2,\cdots,N). \quad (13)$$

Then, Eq.(10) can be rewritten as the follows,

$$(D_{ij}^{(2)} - \alpha^2 - \gamma^2)\frac{d}{dt}\begin{pmatrix}\hat{v}(y_0,t)\\\hat{v}(y_1,t)\\\vdots\\\hat{v}(y_N,t)\end{pmatrix} = g_{ij}\begin{pmatrix}\hat{v}(y_0,t)\\\hat{v}(y_1,t)\\\vdots\\\hat{v}(y_N,t)\end{pmatrix}, \quad (14)$$

where $D_{ij}^{(2)}$ is the differential matrix of the order $(N+1) \times (N+1)$. If the inverse matrix of $(D_{ij}^{(2)} - \alpha^2 - \gamma^2)$ exists, Eq.(14) can be written in,

$$\frac{d}{dt}\hat{v}(y_j,t) = G_{ij}\hat{v}(y_j,t). \quad (15)$$

When the function $\hat{v}$ is expanded by N, Eq.(14) is written in the follows.

$$\frac{d}{dt}\begin{pmatrix}\hat{v}_1(y_0,t)\ldots\hat{v}_N(y_0,t)\\\hat{v}_1(y_1,t)\ldots\hat{v}_N(y_1,t)\\\vdots \quad \vdots \quad \vdots\\\hat{v}_1(y_N,t)\ldots\hat{v}_N(y_N,t)\end{pmatrix} = G_{ij}\begin{pmatrix}\hat{v}_1(y_0,t)\ldots\hat{v}_N(y_0,t)\\\hat{v}_1(y_1,t)\ldots\hat{v}_N(y_1,t)\\\vdots \quad \vdots \quad \vdots\\\hat{v}_1(y_N,t)\ldots\hat{v}_N(y_N,t)\end{pmatrix}. \quad (16)$$

If Eq.(16) is simply described as,

$$\frac{d}{dt}F(t) = G(t)F(t), \quad (17)$$

5

from the Floquet theory, we can expect that the solution of Eq.(17) have the form of,

$$F(t) = e^{Qt}\Phi(t) . \qquad (18)$$

Here $\Phi(t)$ is an arbitrary periodic function with the period T, and Q consists of N Floquet exponents. Because of the character of the periodic function $\Phi(t)$,

$$F(0) = \Phi(0) \equiv I . \qquad (19)$$

Thus,

$$F(T) = e^{QT}\Phi(T) = e^{QT} . \qquad (20)$$

Therefore, the Floquet exponents are obtained as the follows.

$$Q = \frac{1}{T}\ln F . \qquad (21)$$

When the eigenvalues of the matrix Q denote as μ_i and the eigenvalues of F as σ_i, we can obtain the Floquet exponents in the form of,

$$\mu_i = \frac{1}{T}\ln \sigma_i . \qquad (22)$$

Thus, if we know the matrix F, the Floquet exponents are obtained from Eq.(22). In general, the matrix F can be numerically obtained by the integration of Eq.(17) during the period T. In the present study, the Cranc-Nicorson method is employed for this process.

3.3 Results

Figure 8 shows a typical velocity profiles at each 1/8 period of the wall-oscillation. Because of the symmetry, the only lower half is shown. Substituting these profiles into U in Eq.(10), the time-integration of Eq.(17) is executed in order to obtain $F(T)$. Before the parametric study, the calculation of the Floquet exponent was checked by putting U_w in Eq.(2) onto 0. In this case, the Floquet exponent should be equivalent to the eigenvalue of the plane Poiseuille flow. Table 1 shows the comparison of the eigenvalues obtained in the present study with the results by Orszag[1]. It seems that the accuracy of the numerical scheme using here is sufficient.

Result of the parametric study is shown in Fig. 9 as a contour map on Ω-U_w plane. The white color region represent the positive area of the Floquet exponent, which corresponds to the unstable region, and the black one corresponds to the stable one. The dash-dotted lines in this figure are written by each 0.002 of the Floquet exponent, and the solid line represents zero eigenvalue, namely the neutral curve. It can be seen that the stable region exists as a deep crevasse along U_w axis. From the comparison with Fig. 6, the bottom of the stable region agrees well with decelerated region estimated by the DNS. Although the unstable region near the U_w axis also corresponds to each other, some portion of the accelerated region by the DNS exists in the stable crevasse. This discrepancy might come from a reason that DNS can reproduce the nonlinear phenomena. From analogy of the Stokes layer, it can easily speculate that the condition with small Ω is equivalent to with large
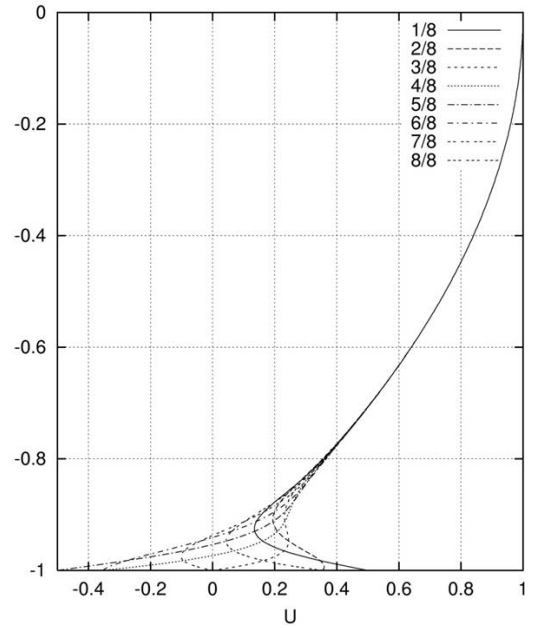

Fig.8 Velocity profiles at some instance.

Table 1 Comparison of the eigenvalues.

	ω_r	ω_i
present	0.23753e+00	0.37397e-02
Orszag[1]	0.23752464	0.00373967

disturbance. Thus some cases estimated as the acceleration by DNS correspond to the transient growth with large disturbances.

4   Conclusion

The effect of longitudinal wall-oscillation on the plane Poiseuille flow is studied by direct numerical simulation (DNS) and the Floquet analysis based on the linear stability analysis. From the DNS, the laminar-turbulent transition is accelerated or decelerated depending on the frequency of the wall-oscillation Ω and its amplitude U_w. In the accelerated case, it is cleared by the flow visualization that the growth of the coherent structure near the walls are suppressed by the wall-oscillation. The result obtained by the Floquet analysis agrees well with the DNS analysis and a deep stable crevasse appears in the parameter space.
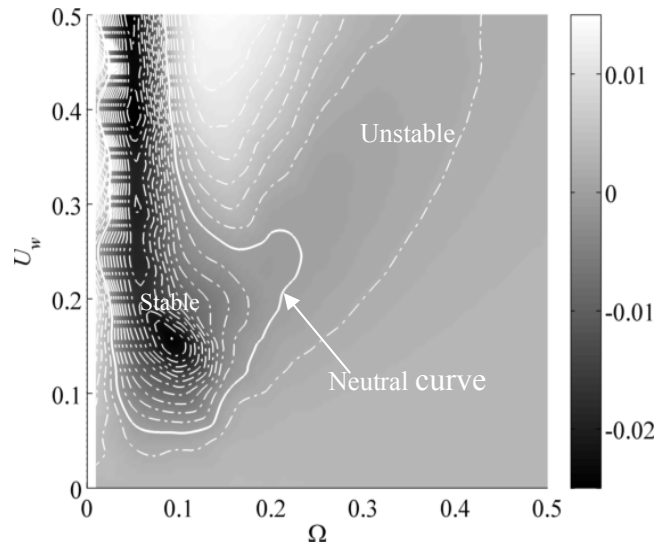

Fig.9 Contour of the Floquet exponent. White color corresponds to the unstable region, and black to the stable one. The solid line represents the neutral curve.

References

[1]   Orszag, S. A.: Accurate Solution of the Orr-Sommerfeld Stability Equation, *J. Fluid Mech.*, **50**, 689 (1971), pp.1441-1447.

[2]   Kim, J., Moin, P., and Moser, R..: Turbulence Statistics in Fully Developed Channel Flow at Low Reynolds Number, *J. Fluid Mech.*, 177 (1987), pp.133-166.

[3]   Selvarajan, S., Tulapurkara, E.G., and Vasanta Ram, V.: Stability Characteristics of Wavy Walled Channel Flows, *Phys. Fluids*, **11** (1999), pp. 579-589.

[4]   Floryan, J. M.: Stability of Wall-Bounded Shear Layers in the Presence of Simulated Distributed Surface roughness, *J. Fluid Mech.,* **335** (1997), pp. 29-55.

[5]   Floryan, J. M., Szumbarski, J., and Vasanta Ram, V.: Stability of a Flow in a Channel with Vibrating Walls, *Phys. Fluids*, **14** (2002), pp. 3927-3936.

[6]   Zhou, H., Martinuzzi, R. J., Khayat, R. E., Straatman, A. G., and AbuRamadan, E.: Influence of Wall Shape on Vortex Formation in Modulated Channel Flow, *Phys. Fluids*, **15**, (2003), pp.3114-3133.

[7]   Choi, H., Moin, P., and Kim, J.: Active Turbulence Control for Drag Reduction in Wall Bounded Flows, J. Fluid Mech., 262 (1994), pp.75-110.

[8]   Sumitani, Y. and Kasagi, N.: Direct Numerical Simulation of Turbulent Transport with Uniform Wall Injection and Suction, AIAA J., 33, (1995), pp.1220-1228.

[9]   Jung, W. J., Mangiavacchi, N., and Akhavan, R.: Suppression of Turbulence in Wall-Bounded Flows by High-Frequency Spanwise Oscillations, Phys. Fluids, A 4 (8) (1992), pp.1605-1607.

[10]   Quadrio, M. and Ricco, P.: Critical Assessment of Turbulnet Drag Reduction Through Spanwise Wall Oscillation, J. Fluid Mech., 521, (2004), pp.251-271.

[11]   Choi, K.-S.: Near-Wall Structure of Turbulent Boundary Layer with Spanwise-Wall Oscillation, Phys. Fluids, 14 (2002), pp.2530-2542.

[12]   Ricco, P. and Quadrio, M.: Wall-Oscillation Conditions For Drag Reduction in Turbulent Channel Flow, Int. J. Heat Fluid Flow, 29 (4) (2008), pp. 891-902.

[13]   Canuto, C., Hussaini, M. Y., Quarteroni, A. and Zang, T. A.: Spectral Methods in Fluid Dynamics, Springer-Verlag, Berlin, 1988.